Appl Microbiol Biotechnol (2002) 58:735–742
DOI 10.1007/s00253-002-0969-9

ORIGINAL PAPER

P. Bruheim · M. Butler · T. E. Ellingsen

A theoretical analysis of the biosynthesis of actinorhodin in a hyper-producing *Streptomyces lividans* strain cultivated on various carbon sources

Received: 31 October 2001 / Received revision: 7 February 2002 / Accepted: 7 February 2002 / Published online: 20 March 2002

Abstract A stoichiometric equation for the biosynthesis of actinorhodin (ACT) was derived taking into consideration both the requirements of the carbon precursors (acetyl-CoA) and reducing power (NADPH). The estimate for reducing power was derived from a detailed molecular analysis of each step in the ACT biosynthetic pathway. Even though ACT is slightly more oxidized than most carbon substrates, e.g. glucose, reducing power (NADPH and NADH) is necessary due to reducing steps and to monooxygenase steps. The equation was used to evaluate, in a metabolic network context, the experimental results from batch fermentations with eight different carbon sources using a *Streptomyces lividans* 1326 derived strain containing the pathway-specific activator gene (*act*II-ORF4) on a multicopy plasmid (pIJ68). The yield of ACT on the various carbon sources ranged from 0.04 to 0.18 Cmol ACT/Cmol carbon source in the stationary phase. Glucose was the best carbon source and supported a yield of 25% of the maximum theoretical yield. There are no obvious constraints in the primary metabolic pathways that can explain why the various carbon sources allowed different levels of ACT production, because their potential for supplying acetyl-CoA and NADPH are far from fully utilized. For the observed ACT yields, there is an excess production of NADPH that has to be reoxidized either by a transhydrogenase or a NADPH oxidase. This study discusses the central metabolic pathways, focusing on providing precursors for ACT synthesis.

P. Bruheim (✉)
Department of Biotechnology, Sem Selands vei 6/8,
Norwegian University of Science and Technology,
Trondheim, Norway
e-mail: Per.Bruheim@chembio.ntnu.no
Tel.: +47-735-92836, Fax: +47-7359-1283

M. Butler
Department of Molecular Microbiology,
John Innes Centre, Norwich, UK

T.E. Ellingsen
Sintef Applied Chemistry, Group of Industrial Biotechnology,
Trondheim, Norway

Introduction

A detailed knowledge of the regulation of secondary metabolite biosynthetic pathways is of critical importance for a rational approach to strain improvement (Chater 1990). This comes in addition to the stringent regulation of primary metabolism. Directed improvement of the production of secondary metabolites by metabolic engineering strategies may therefore be more difficult than for primary metabolites.

Secondary metabolite production in *Streptomyces* is regulated both by pathway-specific activators and pleiotropic regulators. A great deal of work has been aimed at understanding the physiological signals and underlying regulatory mechanisms involved in actinorhodin (ACT) production, especially in *Streptomyces coelicolor* (Bibb 1995). *Streptomyces lividans* is closely related to *S. coelicolor* and carries the genes for ACT biosynthesis, but in most circumstances does not produce this antibiotic. However, a *S. lividans* strain carrying the actinorhodin (ACT)-pathway-specific activator gene (*act*II-ORF4) from *S. coelicolor* on a multicopy plasmid (pIJ68) has been shown to produce large amounts of ACT (Bruheim et al. 2002). A defined minimal medium supporting a high yield of ACT and suitable for physiological studies such as metabolic flux analysis was developed. Over 5 g ACT l^{-1} was produced over 7 days of fermentation and 17% of the carbon substrate was converted to ACT in the stationary phase. Since this constitutes between 20 and 30% of the theoretical maximum in the absence of growth, even higher yields may be obtained by further genetic modification of this strain.

One of the major tasks in metabolic engineering is to identify metabolic targets that can be modified to give a desired metabolic improvement (such as increased productivity of a specific product). There have been few reported studies on metabolic engineering of primary carbon metabolism in *Streptomyces* spp. in spite of their industrial importance. This report focuses on the primary metabolic pathways of carbon utilization and how carbon sources entering central metabolic pathways support

growth, as well as ACT and organic acid production. ACT was chosen as a model system since its biosynthesis and regulation have been the subject of extensive research. Here, we turn to the physiological basis for the interpreting of batch-fermentation results. It is necessary to have a detailed knowledge about the requirements for carbon precursors and reducing equivalents for the biosynthesis of ACT when performing quantitative analysis of the metabolism. Such information is not available for ACT biosynthesis. A biosynthesis equation for ACT is therefore derived here and this equation is used to evaluate the experimental results in a metabolic network context.

Materials and methods

Microorganisms

These studies were carried out with *S. lividans* 1326 and various plasmid-containing derivatives. Strain RpdS 102 is *S. lividans* strain 1326 containing *act*II-ORF4 cloned on a multi-copy plasmid (pIJ68, Passantino et al. 1991); strain RpdS 105 is *S. lividans* containing the vector alone (pIJ486, Kieser et al. 2000), while wild-type *S. lividans* was designated strain RpdS 101. Unless otherwise stated, the plasmids were maintained by selecting for thiostrepton (10 μg ml^{-1}).

Media, growth conditions, and analysis

For detailed protocols regarding the mineral medium and cultivation conditions, refer to Bruheim et al. (2002). The mineral medium (AMM) used was prepared as follows (per liter of distilled water): 9.4 g NH_4Cl, 1.78 g $Na_2HPO_4 \cdot 2H_2O$, 0.2 g $MgCl_2 \cdot 6H_2O$, 0.7 g KCl, 0.85 g Na_2SO_4, 2 g NaCl, 1 ml 0.05 M $CaCl_2$. The medium was supplemented with 2 ml trace mineral solution containing per liter distilled water: 13.5 g $FeCl_3 \cdot 6H_2O$, 1.5 g $CuCl_2 \cdot 2H_2O$, 9 g $ZnCl_2$, 3.6 g $MnCl_2 \cdot 4H_2O$, 0.6 g $Na_2MoO_4 \cdot 2H_2O$, 0.4 g $CoCl_2 \cdot 6H_2O$ and 0.3 g H_3BO_4. Carbon source concentration at the start was 50 g l^{-1}. The concentration of carbon source in the fermentors was kept in the 10–15 g l^{-1} range by pulsing a concentrated solution of carbon source (500 g l^{-1}) when required. A two-stage inoculum protocol was used. Medium for the first stage (per liter of distilled water): 15.0 g glucose, 15.0 g glycerol, 15.0 g soya peptone, 3.0 NaCl, 1.0 g $CaCO_3$, and the second stage: 33.0 g glucose, 15.0 g yeast extract. Mycelial cells in 15% glycerol were stored in cryotubes at –80 °C; 1 ml was used to inoculate the first stage of the inoculum. The cultures were incubated with stirring (400 rpm) for 48 h and 24 h during the first and second stages, respectively, in baffled 500-ml Erlen-Meyer flasks with 150 ml medium. Twelve ml of culture was transferred from stage one to two. Inoculum concentration in the fermentors was 5%. Fermentations were run at 28 °C for 6–7 days in 3-l Applicon fermentors with an operation volume of 1 l. The stirrer speed was set to 900 rpm and the air flow rate at 0.5 vvm. Dissolved oxygen was never below 40% of saturation. Silicon-based antifoam (Union Carbide SAG 5693) was added manually when required. Fermentors were maintained at pH 7.0 by addition of 2 M HCl or 2 M NaOH. CO_2 concentration in the effluent gas was continuously monitored on a Rosemount Binos 100 CO_2 analyzer and subsequently logged together with data for pH, flow, and glucose added in the time period between the sample withdrawals. Oxygen concentration in the effluent gas was measured on a Rosemount Oxynos 200 O_2 analyzer at every sample point. Dry weight (DW) was measured from 10-ml samples of cultures that were centrifuged twice and washed with distilled water before drying at 110 °C for 24 h. ACT content was measured both in the supernatant and in the pellet. The ACT concentration was determined with the standard 1 M KOH assay measuring the absorbance at 640 nm and using the extinction coefficient of 25,320 (Brockmann et al. 1950).

Glucose, gluconic acid, xylose, glycerol and organic acids were analyzed on a Shimadzu LC 9A HPLC with an Aminex-HPX-87H column at 45 °C using 5 mM H_2SO_4 (0.6 ml/ min) as eluent. A Shimadzu RID 6A RI detector and a Shimadzu SPD 6A UV detector were mounted in series. Glucose and α-ketoglutaric acid concentrations were also determined by enzymatic assays, using the glucose oxidase enzymatic kit from Biomeriux and glutamic acid dehydrogenase enzymatic kit from Boehringer Mannheim. Glutamic acid concentration was determined by the same assay by trapping NADH with the reduction of INT. In addition, enzymatic analysis for pyruvic acid and acetate (Boehringer Mannheim) were carried out to confirm the HPLC analysis.

Results and discussion

Batch cultivations of *S. lividans* strain RpdS 102 on various carbon sources

Eight carbon sources (glucose, glycerol, xylose, gluconic acid, glutamic acid, mannose, mannitol, and galactose) were tested for their ability to support growth and ACT production in *S. lividans* strain RpdS 102 (1326 carrying the ACT pathway-specific activator gene *act*II-ORF4). They were chosen on the basis of where they enter the central metabolism. The fermentation data presented in Table 1 A, B are from the stationary phase with highest volumetric ACT production rates and nearly no increase in the biomass. Glucose was included as a reference in both fermentation series. The high-yield medium used in this study, developed in a prior study, is phosphate-limited (Bruheim et al. 2002). The phosphate limitation is reached at the peak of CO_2 production. Every set of fermentation series was repeated at least once and a representative series is presented.

Glucose

Glucose supported the highest yield of ACT. The growth and ACT production curves are presented in Fig. 1 and Table 1 A. Glucose fermentations of *S. lividans* strain RpdS 102 have also been studied extensively earlier (Bruheim et al. 2002). In the stationary phase 17% of the glucose carbon was converted to ACT carbon.

Glycerol

Glycerol supported the fastest growth rate for *S. lividans* strain RpdS 102 with a maximal growth rate at 0.10 h^{-1} at 20–30 h (Fig. 2). The volumetric ACT production was much lower in the late stationary phase (80–140 h) (Table 1 A) than in the early stationary phase (40–60 h) (data not shown). The yield of ACT on glycerol is also much lower in the late (100–140 h) than in the early phase (40–60 h; data not shown). This indicated that a metabolic/carbon flux shift was induced during the early stationary phase, which resulted in a decrease in both

Table 1 Fermentation data for *Streptomyces lividans* strain Rpds 102 using various carbon sources. Data are average values between two sampling times in a stationary phase (except μ_{max}) with constant actinorhodin (ACT) production rates (stationary phase after the increase in cell mass has ended). *DW* Dry weight (g l^{-1}), r_s (mmol $C_{glucose}$/g DW-h), r_c (mmol C_{CO2}/g DW-h), r_{act} (mmol C_{act}/g DW-h), r_k (mmol $C_{\alpha\text{-ketoglutaric acid}}$/g DW-h), r_p (mmol $C_{pyruvic\ acid}$/g DW-h), *RQ* (mol CO_2/mole O_2), Y_{SA} (mol C_{act}/mol $C_{glucose}$). SD±5%

Reactor conditions	DW	μ_{max}[a]	Data from production phase					RQ	Y_{SA}	$Y_{SA}/Y_{theoretical\ max.}$[b]	Recovery (%)
			r_s	r_c	r_{act}	r_k	r_p				
A.											
Glucose	10.8	0.07	1.30	0.92	0.22	0.00	0.00	0.78	0.17	0.25	88
Glycerol[c]	11.5	0.10	0.95	0.60	0.03	0.16	0.06	0.65	0.03	0.04	89
Glutamate	8.6	0.03	1.06	0.92	0.03	0.00	0.00	0.82	0.03	0.05	90
Xylose	14.0	0.04	1.28	0.81	0.14	0.14	0.00	0.75	0.11	0.16	85
Gluconate	10.7	0.07	1.98	1.61	0.13	0.06	0.00	0.84	0.07	0.13	91
B.											
Glucose	11.5	0.07	0.84	0.57	0.15	0.00	0.00	0.79	0.18	0.27	89
Galactose	9.5	0.07	1.12	0.84	0.13	0.00	0.00	0.77	0.12	0.18	87
Mannose	12.0	0.08	1.27	0.98	0.12	0.00	0.00	0.76	0.09	0.13	87
Mannitol	10.0	0.08	1.83	1.43	0.16	0.00	0.00	0.70	0.09	0.13	87

[a] Maximal growth rate in the exponential growth phase
[b] Transhydrogenase active (see Table 2)
[c] Date from late stationary phase. *T*=80–140 h. (see text)

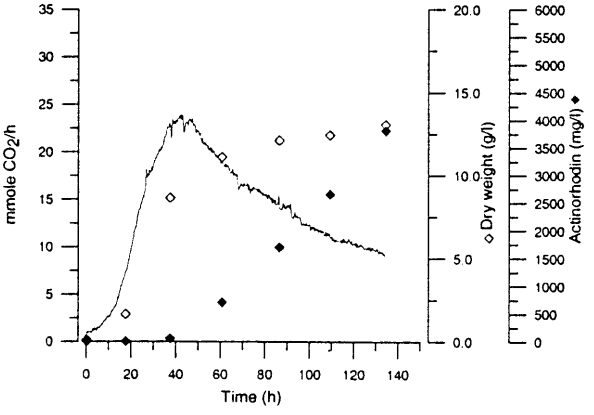

Fig. 1 Time course for growth and ACT production in fed batch fermentation of *Streptomyces lividans* strain RpdS 102 with glucose as carbon source

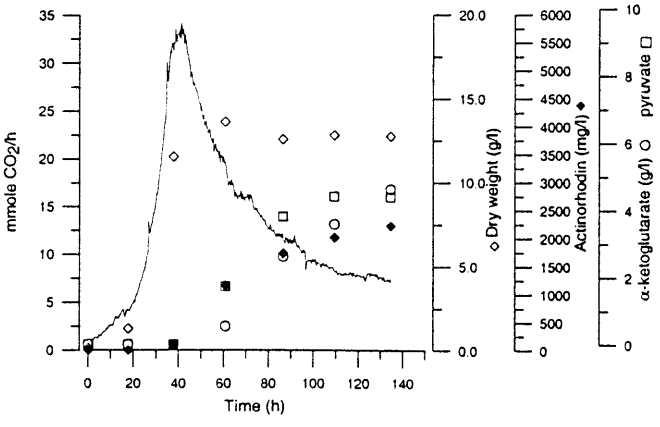

Fig. 2 Time course for growth and ACT production in fed batch fermentation of *S. lividans* strain RpdS 102 with glycerol as carbon source.

volumetric ACT production and ACT yield on glycerol. This particular ACT production profile was observed only for glycerol. α-Ketoglutaric acid and pyruvic acid production were observed in the stationary phase, and also the volumetric acid production decreased in the late phase compared with the early phase.

Glutamic acid

Glutamic acid supported slow growth (μ_{max} 0.03 h^{-1}) even though the increase in CO_2 production rate was the same as for the glucose culture. The final dry weight was significantly lower than with glucose or glycerol. The specific ACT production rate and yield were also low (Table 1 A). However, in contrast to glycerol, there was no excretion of α-ketoglutaric acid or pyruvic acid.

Gluconic acid

Gluconic acid supported a relatively high production of ACT by *S. lividans* strain RpdS 102. There was also a significant production of α-ketoglutaric acid, which was observed after ACT synthesis began. The specific substrate consumption was much higher than for the other carbon substrates (Table 1 A). This high respiratory activity is reflected in the level of CO_2 production, which was maintained in the stationary phase whereas it declined with the other carbon sources.

Xylose

Xylose supported slow growth for *S. lividans* strain RpdS 102. This culture was cultivated for an extra 60 h. The final biomass concentration is significantly higher

for xylose than for glucose. ACT production was high in the late stationary phase (Table 1 A). The yield of ACT on xylose is second best after glucose. α-Ketoglutaric acid production started during growth, in contrast to the cultures grown on glycerol and gluconate, in which acid production started after growth had ceased.

Mannose, galactose, mannitol

Carbon sources that enter primary metabolism at the glucose-6-phosphate node were also tested. Glucose was included as a reference, and although the respiration rate in the stationary phase was lower than in previous fermentations, the yield of ACT on glucose was the same (Table 1 B). Cultures grown on galactose and mannose behaved similarly to those grown on glucose. The specific ACT production rates were almost the same, but the yield was lower due to the higher specific carbon source consumption rate. Mannitol (a more reduced carbon source than the hexoses) supported a higher respiration rate but the ACT yield was the same as for mannose in the stationary phase.

Quantitative information on carbon precursor and cofactor consumption for ACT biosynthesis is required in order to evaluate these results in a metabolic network context. The consumption of carbon precursors compounds and cofactors cannot be directly deduced from the chemical structure of the final metabolite. Instead, a detailed knowledge of each of the individual steps in the biosynthetic pathway is necessary.

Derivation of ACT biosynthesis equation and estimation of maximum theoretical yields

ACT is a polyketide (Fig. 3A) synthesized by a type II polyketide synthase (monofunctional multienzyme complex) carrying out the various condensation, reduction steps, etc., in sequence (Hopwood and Sherman 1990). Malonyl-CoA is the only carbon precursor and 16 molecules are needed for the production of one molecule of ACT (Gorst-Allman et al. 1981). Mutants blocked at various steps of the ACT pathway have been made, and the chemical structures of many of the intermediates have been determined. Based on these studies a tentative pathway with seven intermediate structures has been proposed (Katz and Donadio 1993). Here we present a quantitative theoretical analysis of ACT biosynthesis. The principle for the derivation of the quantitative equation is an elemental and redox balance and an analysis at the molecular level of each step in the ACT biosynthesis pathway (Fig. 3B). Some assumptions about the cofactor dependence of the enzymes in the multienzyme complex have to be made. Malonyl-CoA is assumed to be both starter and elongation moiety (Dreier and Khosla 2000), and ATP is used for the activation of acetyl-CoA to malonyl-CoA by acetyl-CoA carboxylase. ACT is a dimer with the dimerization reaction represented in step 8. The first step, condensation of

A.
Actinorhodin

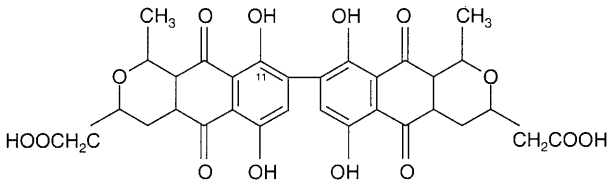

B.
Biosynthesis of actinorhodin in eight steps from acetyl-CoA. Actinorhodin is a dimer with the dimerisation reaction in step 7. For chemical structures of the intermediates see Katz and Donadio (1993)

Activation step: $16CH_3CO\text{-}SCoA + 16CO_2 + 16ATP \rightarrow 16MalCoA$
1. *act*I: $2*[8MalCoA \rightarrow C_{16}H_{17}O_8\text{-}Enz + 8CoASH + 8CO_2]$
2. *act*III: $2*[C_{16}H_{17}O_8\text{-}Enz + NADPH + H_2O \rightarrow C_{16}H_{20}O_9 + CoASH]$
3. *act*VII: $2*[C_{16}H_{20}O_9 \rightarrow C_{16}H_{16}O_7 + 2H_2O]$
4. *act*IV: $2*[C_{16}H_{16}O_7 \rightarrow C_{16}H_{14}O_6 + H_2O]$
5. *act*VI: $2*[C_{16}H_{14}O_6 + 2NADPH \rightarrow C_{16}H_{16}O_5 + H_2O]$
6. *act*VA-orf6: $2*[C_{16}H_{16}O_5 + 0.5O_2 \rightarrow C_{16}H_{14}O_6 + NADH]$
7. *act*VB $2*C_{16}H_{14}O_6 \rightarrow C_{32}H_{26}O_{12} + NADH$
8. *act*VA-orf6: $C_{32}H_{26}O_{12} + 2*0.5O_2 \rightarrow ACT(C_{32}H_{26}O_{14})$

Fig. 3 **A** Structure of ACT. **B** Deduction of biosynthesis equation of ACT from acetyl-CoA

eight malonyl-CoA units to one of two 16-carbon acyl chains in the ACT molecule, is catalyzed by the *act*I locus. Step 2 is a reducing step catalyzed by *act*III in which the keto group at C-9 is reduced and, analogously to the fatty acid condensation/reduction cycle, this reaction is assumed to be NADPH-dependent. Indeed, it has been recently noted (K. Ichinose, University of Tokyo, personal communication) that the *act*III gene product displays homology to tropinone reductases, which have been demonstrated to contain $NADP^+$ by X-ray crystallography (Nakajima et al. 1998). The products of the *act*VII and *act*IV genes catalyze step 3 and 4. These are dehydration reactions. Step 5 is carried out by *act*VI gene products (Ichinose et al. 1997; Taguchi et al. 2000) and appears to involve the overall loss of one oxygen atom in forming the pyran ring. For the *act*VI locus there are two ORFs which both have amino acid sequence motifs characteristics of binding sites for NADPH (Fernandez-Moreno et al. 1994). Four hydrogen are necessary for the redox balancing of step 5, so it is assumed that 2 NADPH are consumed. The monooxygenase reaction catalyzed by *act*VA-ORF6 in step 6 has been shown to operate through an unusual mechanism, which does not require any cofactor (even though it is a redox reaction, Kendrew et al. 1995, 1997). One NADH is added in step 6, presumably produced by oxidation of the hydroxyl to a keto group. Two hydrogen are removed in the dimerization step (step 7) with a net gain of 1 NADH. The last step is also catalyzed by *act*VA-ORF6, but here the enzyme is functioning on the dimer. Since the two hydroxyl groups (one on each monomer) are not oxidized to keto groups, no NADH is formed in this reaction. Therefore, based on this assessment of the eight steps of the ACT biosynthesis pathway the following biosynthesis equation is proposed:

$$16AcCoA + 6NADPH + 16ATP + 2O_2 \rightarrow ACT(C_{32}H_{26}O_{14}) + 3NADH + 16CoASH + 6H_2O$$

Table 2 Calculation of maximum theoretical yield of ACT on various carbon sources based on a deduced ACT biosynthesis equation. *PPP* Pentose phosphate pathway, *TCA* tricarboxylic acid cycle

Carbon source	Maximum theoretical yield of ACT on carbon source Cmol ACT Cmol^{-1} carbon source		
	NADPH from PPP	NADPH from TCA	Transhydrogenase
Glucose, mannose, Galactose, mannitol	0.59	0.48	0.67
Gluconic acid[a]	0.49	0.40	0.67
Xylose	0.59	0.48	0.67
Glycerol	0.59	0.48	0.67
Glutamate[b]	0.40	0.40	0.40

[a] 6-Phosphogluconate dehydrogenase is NAD-dependent. Gluconate maximum theoretical yield is therefore as for xylose included the carbon loss in the decarboxylation to xylose
[b] Glutamate dehydrogenase is NADP-dependent

The degree of reduction (κ) for ACT is 3.94 [calculation based on the definition of Roels (1983)]. This implies that ACT is slightly more oxidized than, for example, glucose (κ=4.0) and acetyl-CoA (κ=4.0). But, reducing power in the form of NADPH is required for the synthesis of ACT according to the evaluation of the biosynthetic pathway in Fig. 3B.

The overall equation for ACT synthesis is: 16 acetyl-CoA→ACT+NADH. This equation is balanced with respect to elements and redox status but it is enzymatically wrong and shows the importance of detailed knowledge of the biosynthetic pathway.

Some uncertainty due to the lack of precise detailed molecular knowledge of the tailoring reactions remains in the estimation of the NADPH demand. The estimate presented here (6 NADPH per ACT molecule) represents the most likely figure (although experimental confirmation of the *act*III requirement for NADPH has not yet been obtained). However, it is clear that relatively much more carbon is consumed for building the carbon skeleton than for the formation of NADPH.

The estimation of ATP consumption is uncertain since steps other than the formation of malonyl-CoA from acetyl-CoA may require ATP. A thermodynamic analysis of the proposed equation showed that the reaction with the hydrolysis of 16 ATP is thermodynamically feasible at standard conditions (Gibbs free energy of formation of ACT was calculated from the individual groups in the ACT molecule, for procedure see Stephanopolous et al. 1998).

In the calculation of maximal theoretical yields of ACT on carbon source, the following assumptions are made. The formation of acetyl-CoA from the various carbon sources provides enough NADH and ATP for cell maintenance. No NADPH is consumed for cell maintenance and there is no biomass increase in the stationary phase. It is necessary to form 6 NADPH in the pentose phosphate pathway (PPP) or alternatively by isocitrate dehydrogenase in the tricarboxylic acid (TCA) cycle or by a transhydrogenase. Glucose-6-phosphate dehydrogenase and isocitrate dehydrogenase were tested and shown to be NADP-dependent while 6-phosphogluconate dehydrogenase was NAD-dependent. This was verified for *S. lividans* cells both in the growth and stationary phases. The maximum theoretical yield of ACT on carbon source for these extreme situations is presented in Table 2. In the case of a transhydrogenase, the NADPH demand is satisfied by the formation of acetyl-CoA from the various carbon sources. The maximum theoretical yield is highest for glucose, mannose, galactose, mannitol, glycerol and xylose. It is somewhat lower for gluconic acid and significantly lower for glutamic acid. Glutamic acid enters into the TCA cycle and gives a lower yield because three out of five carbons are lost as CO_2.

Evaluation of the experimental yields of *S. lividans* strain RpdS 102 in a metabolic network context

A simple bioreaction network for ACT synthesis in the stationary phase (excluding biomass increase) includes substrate uptake, the Embden-Meyerhof pathway (EMP), PPP, pyruvate dehydrogenase, TCA, oxidative phosphorylation and ATP hydrolysis (i.e. no constraint on ATP and NADH), anaplerotic reaction (most likely phosphoenolpyruvate carboxylase in *Streptomyces*) in case of excretion of TCA intermediates and, finally, the proposed biosynthetic equation of ACT (Fig. 4).

NADPH is formed both in the TCA cycle and the PPP (2 NADPH/glucose oxidized to CO_2 in the TCA cycle and 6 NADPH/glucose oxidized to CO_2 in the PPP). CO_2, H_2O and ACT are the only products formed (when glucose is used as carbon source). So ACT would be the only obvious NADPH sink to consume the NADPH that is produced in the PPP and TCA cycle. However, the NADPH generated by glucose oxidation to CO_2 greatly exceeds what would be required or consumed by the observed ACT production [$r_{c=}$0.92 mmol CO_2/(g DW-h) implying that >0.31 mmol NADPH (0.92·(2NADPH/glucose)/(6 carbons/glucose) is produced per (g DW-h) vs r_{act}=0.22 mmol C_{act}/(g DW-h) implying 0.04 NADPH is consumed/(g DW-h)]. This means that the cells must have an active way of avoiding accumulation of NADPH, e.g. *S. lividans* strain 1326 produced no ACT in the stationary phase but was respiring very actively, implying that NADPH accumulation was not taking place (Bruheim et al. 2002). The metabolic solution for

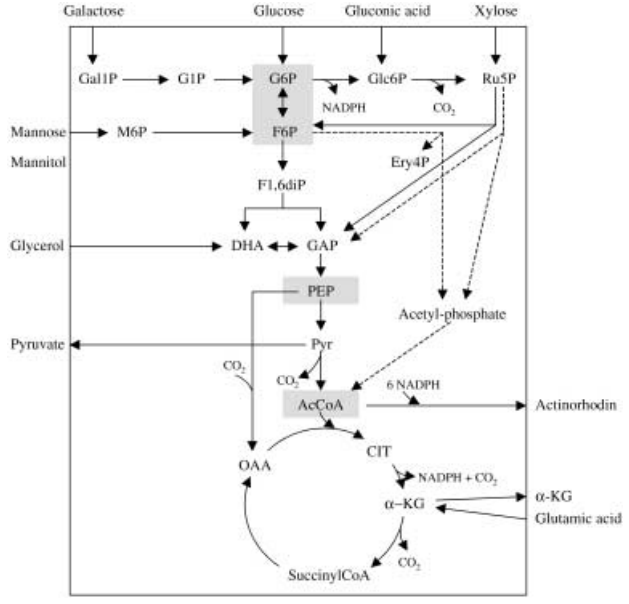

Fig. 4 Metabolic network for biosynthesis of ACT by *Streptomyces lividans*

this "low" yield situation may be the presence of a transhydrogenase. This enzyme catalyzes the transfer of reducing equivalents between NADPH and NADH. The direction of the reaction depends on the ($NADPH/NADP^+$):($NADH/NAD^+$) ratios. In a study by Anderlund et al. (1999) using a membrane-bound *E. coli* transhydrogenase, it was shown that the enzyme worked in the direction of reoxidizing NADPH. Conversely, in another study with a cytoplasmic *Azotobacter vinelandii* transhydrogenase, the enzyme was observed to function in the opposite direction (Nissen et al. 2001). But, no transhydrogenase activity was detected in the *S. lividans* strains (using the protocol by Phelps and Hatefi [(1981), and later, Park et al. (1997) for *Corynebacterium glutamicum*; data not shown]. However, the *S. coelicolor* database (http://www.sanger.ac.uk/Projects/S_coelicolor/) was searched with the *Mycobacterium tubercolosis* membrane-bound transhydrogenase subunit genes *pnt*A and *pnt*B. One cosmid (accession number al450289) was found, with two adjacent ORFs showing 52 and 44% identity to *M. tubercolosis pnt*A and *pnt*B, respectively. So there is little doubt that there is a membrane-bound transhydrogenase in *S. coelicolor,* but the physiological significance of such an activity in *S. lividans* remains to be established. One other theoretical possibility (which has been experimentally excluded in this work in *Streptomyces lividans*) is a NAD-dependent isocitrate dehydrogenase which might have been used to modulate NADPH concentration, e.g. induced at NADPH accumulation to avoid NADPH accumulation if the PPP flux is simultaneously turned down. A NADPH oxidase may also be operative to prevent excessive accumulation of NADPH.

Daae and Ison (1999) presented a primary metabolic network for *S. lividans*, but they assumed in their stoichiometric model that isocitrate dehydrogenase was NAD-dependent, which is not the case as shown in the present study. Naemimpoor and Mavituna (2000) carried out metabolic flux analysis on the *S. coelicolor* data of Melzoch et al. (1997). The reactions in the network were not given, and only the carbon precursor consumption was mentioned for ACT biosynthesis. Their flux estimates would be different if NADPH consumption for ACT biosynthesis were included. Their results also strongly depend (as for Daae and Ison 1999) upon the use of the NADP-NADPH constraint, which may not be a valid constraint as shown in the present study.

A stoichiometric model must be verified by careful analysis of the enzymes both in the reactions of primary and secondary metabolism. However, not all reactions in central metabolism might be identified. For example, in the *S. coelicolor* database there is an ORF with 49% identity to *Bifidobacterium bifidum* phosphoketolase. This enzyme either catalyzes the reaction fructose-6-phosphate to acetyl-phosphate and erythrose-4-phosphate or the reaction xylulose-5-phosphate to acetyl-phosphate and glyceraldehyde-3-phosphate. Acetyl-phosphate can be converted to acetyl-CoA, the precursor for ACT synthesis. This reaction might as well be included in a theoretical model for *S. lividans* (dashed lines in Fig. 4). The use of labeled substrates can (in combination with material balancing) enables a more detailed and reliable analysis of the metabolic network (Christensen and Nielsen 1999).

Glycerol was tested as carbon source for the wild-type strain (*S. lividans* strain RpdS 105) carrying the vector (pIJ486). No ACT production was observed, but both pyruvic acid and α-ketoglutaric acid were secreted at the same level as in *S. lividans* strain RpdS 102 (data not shown). The acid production on glycerol is therefore independent of ACT production. Earlier it had been shown that the high acid production on glucose under nitrogen-limited conditions is also independent of ACT production (Bruheim et al. 2002). The acid and ACT production are therefore unrelated. However, there will be a quantitative relationship between the acid and ACT production through the competition for the common substrate acetyl-CoA, e.g. on glycerol for each Cmol α-ketoglutaric acid produced, enough NADPH was produced by isocitrate dehydrogenase to support a six times higher production of ACT than observed. Further, the carbon flux to acetyl-CoA must be as high as the flux through the anaplerotic reaction during α-ketoglutarate production. So there is no obvious limitation in either acetyl-CoA or NADPH supply. Therefore, ACT yield on glycerol cannot be explained by limitations in the primary metabolic network. Neither is there any obvious reason why the carbon sources entering at the glucose-6-phosphate/fructose-6-phosphate node should support ACT production with such large variation. Further studies with mutant strains in which both the primary metabolism and the regulation of secondary metabolism have been modified are ongoing (manuscripts in preparation). The affinity of the ACT polyketide synthase (i.e. assum-

ing the first step is acetyl-CoA carboxylase) vs citrate synthase for acetyl-CoA and physiological inhibitors and stimulators of the two enzymes are also important. Overexpression of both acetyl-CoA carboxylase and *act*II-ORF4 would for example be an interesting situation to study. This information should be relevant to other secondary metabolite processes, which use acetyl-CoA as a precursor, especially polyketides.

Acknowledgements Financial support was received from EU Cell factory grant BIO4960332 and was coordinated by Dr. R. Luiten. Professors K.F. Chater, D.A. Hopwood, J. Nielsen and Dr. K. Ichinose are thanked for careful reading and valuable comments to the manuscript.

Appendix

Reaction list

Uptake reactions

1. Glucose+ATP→Glucose-6-phosphate
2. Galactose+ATP→Galactose-1-phosphate→→ Glucose-6-phosphate
3. Mannose+ATP→Mannose-6-phosphate→Fructose-1-phosphate
4. Mannitol+ATP→Mannitol-6-phosphate
   Mannitol-6-phosphate → Fructose-6-phosphate+NADH
5. Gluconate+ATP→6-phosphogluconate
6. Xylose→Xylulose
   Xylulose+ATP→Xylulose-5-phosphate→Ribulose-5-phosphate
7. Glycerol+ATP→Glycerol-3-phosphate
   Glycerol-3-phosphate→Dihydroxyacetonephosphate+NADH
8. Glutamate→α-ketoglutarate+NH_3+NAD(P)H

Embden-Meyerhof pathway, pentose-phosphate pathway, tricarboxylic acid cycle

9. Glucose-6-phosphate→Fructose-6-phosphate
10. Fructose-6-phosphate+ATP→Fructose-1,6-diphosphate
11. Fructose-1,6-diphosphate→Dihydroxyacetonephosphate+glyceraldehyde-3-phosphate
12. Dihydroxyacetonephosphate→Glyceraldehyde-3-phosphate
13. Glyceraldehyde-3-phosphate→Pyruvate+2ATP+NADH
14. Pyruvate→AcetylCoA+NADH+CO_2
15. AcetylCoA+oxaloacetate→Citrate
16. Citrate→α-Ketoglutarate+NADPH+CO_2
17. α-Ketoglutarate→Succinyl-CoA+NADH
18. SuccinylCoA→Oxaloacetate+ATP+2NADH
19. Glucose-6-phosphate→6-Phosphogluconate+NADPH
20. 6-Phosphogluconate→Ribulose-5-phosphate+NADPH
21. 3 Ribulose-5-phosphate→2 Fructose-6-phosphate+glyceraldehyd-3-phosphate
22. Phosphoenolpyruvate+CO_2→Oxaloacetate

Excretion reactions

23. Pyruvate→PyruvateEx
24. α-Ketoglutarate→α-ketoglutarateEx
25. 16 AcetylCoA+6 NADPH+16 ATP+2 O_2→Actinorhodin+3 NADH

Oxidative phosphorylation

26. NADH→2 ATP

Transhydrogenase

27. NADPH↔NADH

Phosphoketolase

28. Fructose-6-phosphate→Acetyl-phosphate+erythrose-4-phosphate
29. Xylulose-5-phosphate→Acetyl-phosphate+glyceraldehyde-3-phosphate
30. Acetyl-phosphate→AcetylCoA+P_i

References

Anderlund M, Nissen TL, Nielsen J, Villadsen J, Rydstrom J, Hahn-Hagerdal B, Kielland-Brandt MC (1999) Expression of the *Escherichia coli pntA* and *pntB* genes, encoding nicotinamide nucleotide transhydrogenase, in *Saccharomyces cerevisiae* and its effect on product formation during anaerobic glucose fermentation. Appl Environ Microbiol 65:2333–2340

Bibb M (1995) The regulation of antibiotic production in *Streptomyces coelicolor* A3(2). Microbiology 142:1335–1344

Brockmann H, Pini H, v. Plotho O (1950) Actinorhodin. Chemische Berichte 88:161

Bruheim P, Sletta H, Bibb MJ, White J, Levine DW (2002) High yield actinorhodin production in fed-batch cultivations by a *Streptomyces lividans* mutant overexpressing the pathway-specific regulatory gene *act*II-ORF4. J Ind Microbiol Biotechnol (in press)

Chater KF (1990) The improving aspects for yield increase by genetic engineering in antibiotic-producing streptomycetes. Biotechnology, 8:115–121

Christensen B, Nielsen J (1999) Metabolic network analysis: a powerful tool in metabolic engineering. Adv Biochem Eng Biotechnol 66:209–231

Daae EB, Ison AP (1999) Classification and sensitivity analysis of a proposed primary metabolic reaction network for *Streptomyces lividans.* Metab Eng 1:153–165

Dreier J, Khosla C (2000) Mechanistic analysis of Type II polyketide synthase. Role of conserved residues in the β-ketoacyl synthase-chain length factor heterodimer. Biochemistry 39: 2088–2095

Fernandez-Moreno MA, Martinez E, Caballero JL, Ichinose K, Hopwood DA, Malpartida F (1994) DNA sequence and functions of the *act*VI region of the actinorhodin biosynthetic gene

cluster of *Streptomyces coelicolor* A3(2). J Biol Chem 269: 24854–24863

Gorst-Allman CP, Rudd BAM, Chang C, Floss HG (1981) Biosynthesis of actinorhodin. Determination of the point of dimerisation. J Org Chem 46:455–456

Hopwood DA, Sherman DH (1990) Molecular genetics of polyketides and its comparison to fatty acid biosynthesis. Annu Rev Genet 24:37–66

Ichinose K, Taguchi T, Bedford D, Ebizuka Y, Hopwood DA (1997) Functional complementation of pyran ring formation in actinorhodin biosynthesis in *Streptomyces coelicolor* A3(2) by ketoreductase genes for granaticin biosynthesis. J Bacteriol 183:3247–3250

Katz L, Donadio S (1993) Polyketide synthesis: prospects for hybrid synthesis. Annu Rev Microbiol 47:875–912

Kendrew SG, Harding SE, Hopwood DA, Marsh ENG. (1995) Identification of a flavin:NADH oxidoreductase involved in the biosynthesis of actinorhodin. J Biol Chem 270:17339–17343

Kendrew SG, Hopwood DA, Marsh E, Neil G (1997) Identification of a monooxygenase from *Streptomyces coelicolor* A3(2) involved in biosynthesis of actinorhodin: purification and characterization of the recombinant enzyme. J Bacteriol 179: 4305–4310

Kieser T, Bibb MJ, Buttner MJ, Chater KF, Hopwood DA (2000) Practical streptomyces genetics. John Innes Foundation, Norwich, UK

Naeimpoor F, Mavituna F (2000) Metabolic flux analysis in *Streptomyces coelicolor* under various nutrient limitations. Metab Eng 2:140–148

Nakajima K, Yamashita A, Akama H, Nakatsu T, Hashimoto T, Oda J, Yamada Y (1998) Crystal structure of two tropinone reductases: different reaction specificities in the same protein fold. Proc Natl Acad Sci USA 95:4876–4881

Nissen TL, Anderlund M, Nielsen J, Villadsen J, Kielland-Brandt MC (2001) Expression of cytoplasmic transhydrogenase in *Saccharomyces cerevisiae* results in formation of 2-oxoglutarate due to depletion of NADPH pool. Yeast 18:19–32

Melzoch K, Teixera de Mattos MJ, Neijssel OM (1997) Production of actinorhodin by *Streptomyces coelicolor* A3(2) grown in chemostat culture. Biotechnol Bioeng 54:557–582

Park SM, Sinskey AJ, Stephanpolous G (1997) Metabolic and physiological studies of *Corynebacterium glutamicum* mutants. Biotechnol Bioeng 55:864–879

Passantino R, Puglia AM, Chater KF (1991) Additional copies of the *act*II regulatory gene induce actinorhodin production in pleitropic *bld* mutants of *Streptomyces coelicolor* A3(2). J Gen Microbiol 137:2059–2064

Phelps DC, Hatefi Y (1981) Inhibition of the mitochondrial nicotinamide nucleotide transhydrogenase by dicyclohexylcarbodiimide and diethylpyrocarbonate. J Biol Chem 256:8217–8221

Roels JA (1983) Energetics and kinetics in biotechnology. Elsevier, Amsterdam

Stephanopolous G, Nielsen J, Aristodou A. (1998) Metabolic engineering. Associated, San Diego, California

Taguchi T, Itou K, Ebizuka Y, Malpartida F, Hopwood DA, Surti CM, Milburn KI, Stephenson GR, Ichinose K (2000) Chemical characterization of disruptants of the *Streptomyces coelicolor* A3(2) *act*VI genes involved in actinorhodin biosynthesis. J Antibiot 53:144–152